Manual and Automated Media and Intima Thickness Measurements of the Common Carotid Artery

Christos P. Loizou, *Member, IEEE*, Constantinos S. Pattichis, *Senior Member, IEEE*, Andrew N. Nicolaides, and Marios Pantziaris

Abstract—The intima-media thickness (IMT) of the common carotid artery (CCA) is widely used as an early indicator of the development of cardiovascular disease (CVD). It was proposed but not thoroughly investigated that the media layer (ML) thickness (MLT), its composition, and its texture may be indicative of cardiovascular risk and for differentiating between patients with high and low risk. In this study, we investigate an automated method for segmenting the ML and the intima layer (IL) and measurement of the MLT and the intima layer thickness (ILT) in ultrasound images of the CCA. The snakes segmentation method was used and was evaluated on 100 longitudinal ultrasound images acquired from asymptomatic subjects, against manual segmentation performed by a neurovascular expert. The mean ± standard deviation (sd) for the first and second sets of manual and the automated IMT, MLT, and ILT measurements were 0.71 ± 0.17 mm, 0.72 ± 0.17 mm, 0.67 ± 0.12 mm; 0.25 ± 0.12 mm, 0.27 ± 0.14 mm, 0.25 ± 0.11 mm; and 0.43 ± 0.10 mm, 0.44 ± 0.13 mm, and 0.42 ± 0.10 mm, respectively. There was overall no significant difference between the manual and the automated IMC, ML, and IL segmentation measurements. Therefore, the automated segmentation method proposed in this study may be used successfully in the measurement of the MLT and ILT complementing the manual measurements. MLT was also shown to increase with age (for both the manual and the automated measurements). Future research will incorporate the extraction of texture features from the segmented ML and IL bands, which may indicate the risk of future cardiovascular events. However, more work is needed for validating the proposed technique in a larger sample of subjects.

I. Introduction

CARDIOVASCULAR disease (CVD), including coronary artery disease, cerebrovascular disease, and peripheral artery disease, is the third leading cause of death and adult disability in the industrial world after heart attack and cancer (as reported by the World Health Organization). According to [1], 80 million American adults, of whom about half are estimated to be age 65 or older,

have one or more types of CVD. Of all the deaths caused by CVD among adults aged 20 and older, an estimated 13 millions are attributed to coronary heart disease and to stroke, with atherosclerosis as the underlying cause. A recent study by the World Health Organization estimates that by 2015, 20 million people will die from cerebrovascular disease (mainly from heart attack and stroke).

Atherosclerosis causes thickening of the artery walls and the intima-media thickness (IMT), as shown in Fig. 1(a), is used as a validated measure for the assessment of atherosclerosis [2]. Specifically, an increased IMT is correlated with an augmented risk of brain infarction or cardiac attack [3]. Moreover, the presence of carotid plaques has been correlated not only to CVD, but also to degenerative pathologies such as vascular dementia and Alzheimer's disease [4]. Hence, the assessment of carotid wall status is also essential for early identification of risk conditions in asymptomatic patients. Traditionally, the IMT is measured by manual delineation of the intima and the adventitia layers [2]; see Fig. 1(a), interfaces I5 and I7. Manual tracing of the lumen diameter, as shown in Fig. 1(a), Z4, and the IMT by human experts requires substantial experience, it is time consuming, and results vary according to the training, experience, and subjective judgment of the experts. The manual measurements suffer therefore from considerable inter- and intra-observer variability [2]–[10].

In the last 20 years, several automated techniques for the segmentation and measurement of the IMT from longitudinal ultrasound images of the common carotid artery (CCA) have been developed [9]–[12]. However, there are no studies published in the literature reporting both the manual and the automated segmentation and measurement of the media layer (ML) and the intima layer (IL) of the CCA in ultrasound imaging. Only 3 studies in the literature reported manual measurements of the media layer thickness (MLT) [8], [13], [14]. Earlier research showed that the MLT in peripheral arteries does not change significantly with age and that it ranges from 125 μm to 350 μm [8]. In [13] manual measurements of the thickness of the CCA, IMT and MLT were carried out by an expert on 100 subjects aged 70 years old. In this study [13], it was shown that subjects with CVD (coronary heart disease, myocardial infarction, or stroke) had a significantly thinner ML and a thicker IL than healthy subjects. Furthermore, in [14], the IMT, MLT, and ILT of 90 healthy subjects (aged between 10 and 90 years) were manually measured at their radial and anterior tibial arteries. It was
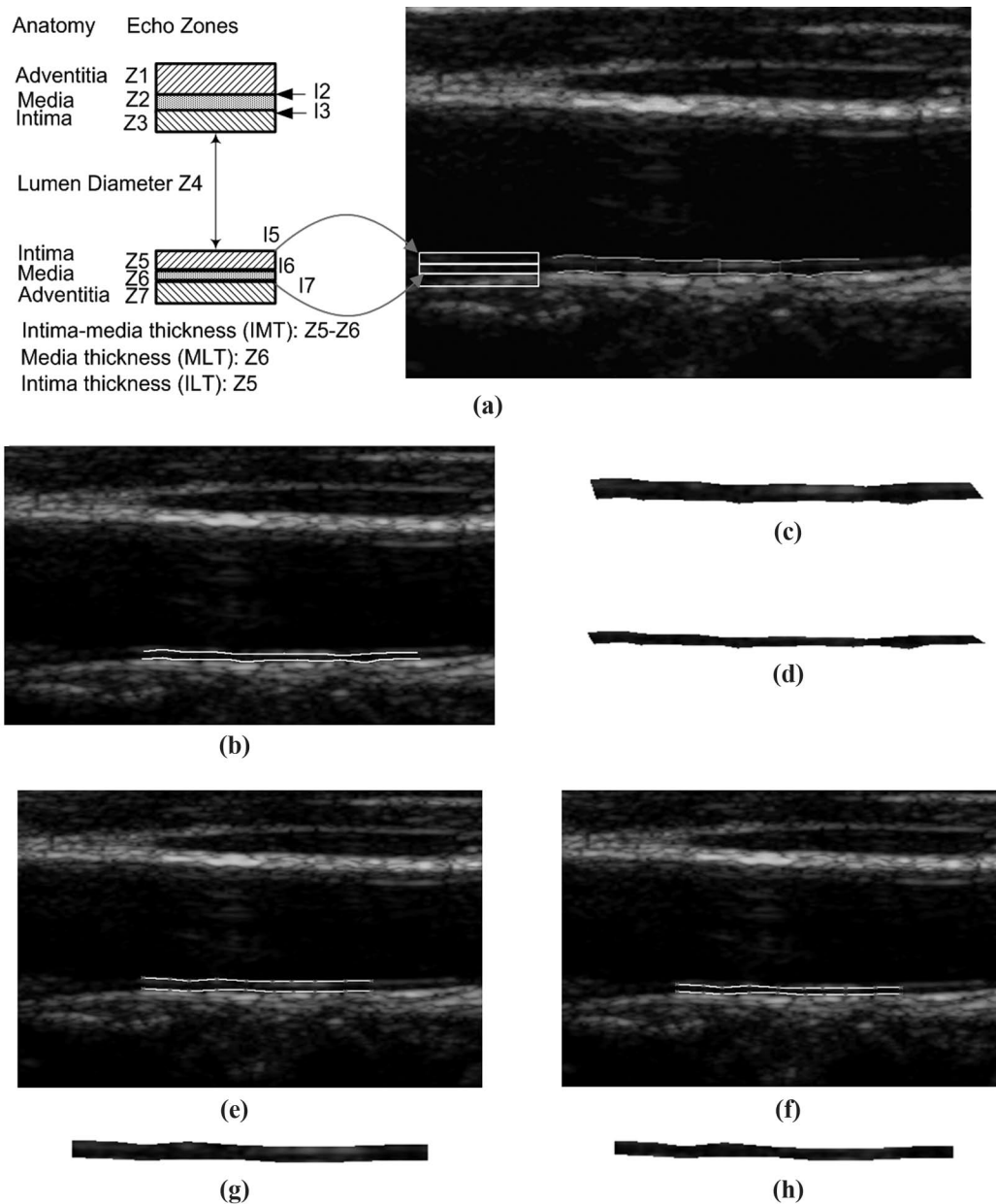
Fig. 1. (a) Illustration of the intima-media-complex (IMC, bands Z5 and Z6) of the far wall of the common carotid artery and the automatic IMC segmentation [10]. The media layer thickness (MLT) is defined as the distance between the intima-media and the media-adventitia interface (band Z6), (b) automated media layer (ML) detection, (c) automated extracted IMC band, (d) automated extracted ML, (e) manual IMC delineation, (f) manual ML delineation, (g) manual extracted IMC, and (h) manual extracted ML.

shown that age was strongly related with IMT, MLT, and ILT for both peripheral arteries.

The objective of this study was to develop and evaluate a snakes segmentation system enabling the automated segmentation and measurement of the ML and IL in ultrasound images of the CCA and investigate their variability with age groups.

The ML, as shown in Fig. 1(a), band Z6, is ultrasonographically characterized by an echolucent region, predominantly composed of smooth muscle cells of the media band of the arterial wall and probably by the extra cellular matrix of the intima band, which cannot be distin-

guished from the smooth muscle cell with ultrasound [15]. Due to the acoustic impedance mismatches, the arterial wall bands (intima-media-adventitia) can produce typical bright-dark-bright patterns on ultrasound images [2]. It is furthermore proposed but not thoroughly investigated, that not only the IMT but rather the ML (its composition and thickness) may be used for evaluating the risk of a patient to develop a stroke and account in general for the risk of the CVD by differentiating between patients with high and low risk.

The IL is a thin layer, the thickness of which increases with age, from a single cell layer at birth to 250 μm at the

age of 40 for nondiseased individuals [5]. Further adaptive physiological thickening of the IL occurs at places where the wall tension is increased, such as arterial bifurcations and on the ML of the artery and may be either eccentric or diffuse [5]. Furthermore, the intima media complex (IMC), as shown in Fig. 1(a), becomes more difficult to detect as the age of patients increases, due to the presence of acoustic holes (echo-dropouts) in the IL [6]. The intimal band, as shown in Z5 in Fig. 1(a), may appear as a thin low contrast structure, and therefore it is difficult to draw boundaries reliably, because smoothing can move the structure edges or make them disappear [2], [7].

Preliminary findings for the segmentation of the ML and MLT were also published in [16] as an extended abstract in the EMBEC Proceedings. The paper is organized as follows. In Section II, materials and methods are given; in Section III, the results are presented; and Sections IV and V include the discussion and the concluding remarks and future work, respectively.

II. MATERIALS AND METHODS

A. Recording of Ultrasound Images

A total of 100 B-mode longitudinal ultrasound images of the CCA used for the IMC, ML, and IL segmentations were recorded using the ATL HDI-3000 ultrasound scanner (Advanced Technology Laboratories, Seattle, WA), with a linear probe (L74), with a recording frequency of 7 MHz, a velocity of 1550 m/s, and 1 cycle per pulse, which resulted in a wavelength (spatial pulse length) of 0.22 mm and an axial system resolution of 0.11 mm. The technical characteristics of the ultrasound scanner (multi-element ultrasound scan head, operating frequency, acoustic aperture, and transmission focal range) have already been published in [10]. Digital images were resized using the bicubic method to a standard pixel density of 16.66 pixels/mm with a resolution of 0.06 mm. This was carried out due to the small variations in the number of pixels per mm of image depth (i.e., for deeply situated carotid arteries, image depth was increased, and therefore, digital image spatial resolution would have decreased) and to maintain uniformity in the digital image spatial resolution [17]. The images were logarithmically compressed and were recorded digitally on a magneto optical drive at 768×576 pixels with 256 gray levels. The images were recorded at the Cyprus Institute of Neurology and Genetics, in Nicosia, Cyprus, from 42 female and 58 male asymptomatic subjects aged between 26 and 95 years old, with a mean age of 54 years. The images were separated into 3 different age groups depending on age, namely, below 50, 50 to 60, and above 60 years old, with 27, 36, and 37 subjects in each group, respectively. These subjects had not developed clinical symptoms, such as a stroke or a transient ischemic attack (TIA).

B. Image Normalization

Brightness adjustments of ultrasound images were carried out in this study based on the method introduced in [18] and also used in [10]. It was shown that this method improves image compatibility by reducing the variability introduced by different gain settings, different operators, and different equipment, and it facilitates ultrasound tissue comparability. Algebraic (linear) scaling of the image was performed by linearly adjusting the image so that the median gray level value of the blood was 0 to 5, and the median gray level of the adventitia (artery wall) was 180 to 190 [18]. The scale of the gray level of the images ranged from 0 to 255. Thus, the brightness of all pixels in the image was readjusted according to the linear scale defined by selecting the 2 reference regions. It is noted that a key point for maintaining a high reproducibility was to ensure that the ultrasound beam was at right angles to the adventitia, adventitia was visible adjacent to the plaque, and, for image normalization, a standard sample consisting of the half of the width of the brightest area of adventitia was obtained.

C. Manual Measurements

A neurovascular expert delineated manually (using the mouse) the IMC [10], ML, and IL on 100 longitudinal ultrasound images of the CCA after image normalization. The IMC was measured by selecting 20 to 40 consecutive points for the intima, as shown in Fig. 1(a), interface I5, and the adventitia, as shown in Fig. 1(a), interface I7, layers. The ML was measured, as shown in Fig. 1(a), band Z6, by selecting 10 to 20 consecutive points for the media, as shown in Fig. 1, interface I6, and the adventitia layers at the far wall of the CCA. The IL, as shown in Fig. 1(a), band Z5, was then derived by subtracting the ML from the IMC. The manual delineations were performed using a system implemented in Matlab (MathWorks, Natick, MA) from our group. The measurements were performed between 1 and 2 cm proximal to the bifurcation of the CCA on the far wall [10] over a distance of 1.5 cm starting at a point 0.5 cm and ending at a point 2.0 cm proximal to the carotid bifurcation. The bifurcation of the CCA was used as a guide, and all measurements were made from that region. The IMT, MLT, and the ILT were then calculated as the average of all the measurements. The measuring points and delineations were saved for comparison with the snakes segmentation method. Two sets of measurements were carried out by the neurovascular expert with a 6 mo interval. All sets of manual segmentation measurements were performed by the expert in a blinded manner, both with respect to identifying the subject and delineating the image.

D. IMC, ML, and IL Snakes Segmentation

A total of 100 ultrasound images of the CCA were segmented to identify IMC, ML, and IL. Segmentation was

carried out after image normalization using the automated snakes segmentation system proposed and evaluated on ultrasound images of the CCA in [10], which is based on the Williams and Shah [19] snake. Initially, the IMC was segmented by a snake segmentation system as proposed in [19], where the boundaries I5 (lumen-intima interface) and I7 (media-adventitia interface) were extracted. Details about the implementation of the algorithm can be found in [10].

The upper side of the ML (see Fig. 1, Z6) was estimated by deforming the lumen-intima interface (boundary I5) by 0.36 mm (6 pixels) downward and then deformed by the snakes segmentation algorithm proposed in [10] to fit to the media boundary; see Fig. 1(a), interface I6). This displacement of 0.36 mm is based on the observation that the manual mean IMT (IMT$_{\text{mean}}$) is 0.71 mm (12 pixels) and lies between 0.54 mm (minimum or 9 pixels) and 0.88 mm (maximum or 15 pixels) [10]. Therefore, the displacement of the contour to estimate the media should be on average 0.36 mm (6 pixels times 0.06 mm) downward, which is half the size of the IMT (the distance between I5 and I7, where I7 is the media-adventitia interface).

To achieve standardization in extracting the thickness of IMC, ML, and IL, segments with similar dimensions were divided based on the following procedure. A region of interest of 9.6 mm (160 pixels) in length, located 1 to 2 cm proximal to the bifurcation of the CCA on the far wall, was extracted. This was done by estimating the center of the IMC area and then selecting 4.8 mm (80 pixels) left and 4.8 mm (80 pixels) right of the center of the segmented IMC. The selection of the same ML area in length from each image is important to be able to make comparable measurements between images and patient groups.

The novelty of the proposed methodology lies in the algorithmic integrated approach that facilitates the automated segmentation and measurements of IL and ML.

E. Statistical Analysis

We computed the mean and median values for the IMT (IMT$_{\text{mean}}$, IMT$_{\text{median}}$), the MLT (MLT$_{\text{mean}}$, MLT$_{\text{median}}$), and the ILT (ILT$_{\text{mean}}$, ILT$_{\text{median}}$), the interobserver error for the IMT, MLT, and the ILT $\left(\text{se} = \sigma/\sqrt{2} \right)$ [9] as well as the IMT ratio [13] (IMT$_{\text{ratio}}$ = MLT/ILT). We also calculated the coefficient of variation, CV%, for the IMT, MLT, and ILT, respectively, which describes the difference as a percentage of the pooled mean values, where for the media CV%$_{\text{Media}}$ = (se$_{\text{Media}}$ × 100)/MLT$_{\text{Media}}$ [9]. The above measurements were also computed for the 3 different age groups, namely, below 50, between 50 and 60, and above 60 years old and for the male and female subjects. Additionally, to assess the intraobserver variability for the neurovascular expert, the manual MLT measurements were repeated 6 mo after the first set of measurements.

The Wilcoxon rank sum test, which calculates the difference between the sum of the ranks of 2 dependent samples, was also used to identify if a significant (S) or a nonsignificant (NS) difference exists at $P < 0.05$ between the manual and the snakes segmentation measurements of IMC, ML, IL and the IMT$_{\text{ratio}}$ for all 100 images, and between the manual and automated segmentation measurements IMC, ML, and IL for the 3 different age groups (below 50, between 50 and 60, and above 60 years old). Furthermore, the Mann Whitney rank sum test was applied to identify differences between male and female subjects. Also, the correlation coefficient, ρ, between the manual and the automated IMT, MLT, and ILT measurements, was investigated, which reflects the extent of a linear relationship between 2 data sets [20].

To investigate how the automated media snakes segmentation method differs from the manual delineation results, we investigated the regression lines for the mean values of the MLT versus age. Regression analysis was also used to demonstrate the relationship between the IMT, MLT, and ILT mean manual measurements and age of the subjects. Bland Altman plots [21], with 95% confidence intervals, were also used to further evaluate the agreement between the manual and the automated media segmentation measurements. The results of this analysis, however, are not presented in this study nor are the results from the expansion of the study published in [10]. Furthermore, box plots for the manual and the automated IMT, MLT, and ILT mean measurements were plotted, as well as for the manual IMT, MLT, and ILT measurements for the 3 different age groups (below 50, between 50 and 60 and above 60 years old).

III. Results

Fig. 1 illustrates an original normalized ultrasound image of the carotid artery with (a) and (b) the automated segmentation of the IMC and ML, (c) and (d) the extracted automated IMC and ML bands, (e) and (f) the manual delineations of the IMC and ML, and (g) and (h) the extracted manual IMC and ML bands, respectively. It should be noted that the size of the IMC and ML areas presented in Fig. 1(c), (d), (g), and (h) is larger than its original size (enlarged to 300 × 20 pixels to be better visualized) and does not represent the original size (see also Section II-D).

The manual (first and second set of measurements) and the automated mean and the median measurements for all 100 images and for the 3 different age groups of the IMC, ML, and IL are presented in Table I, as well as the interobserver error (se), the coefficient of variation (CV%), and the IMT$_{\text{ratio}}$. Table I shows that the mean plus/minus standard deviation for the manual first set and the automated IMT measurements at time zero were 0.71 ± 0.17 mm and 0.67 ± 0.12 mm; for the manual first set and the automated MLT, measurements were 0.25 ± 0.12 mm and 0.25 ± 0.11 mm; and for the manual first set and the automated ILT, measurements were 0.43 ± 0.10 mm and 0.42 ± 0.13 mm, respectively. The interobserver error (se), for the manual first set and the automated IMT segmentation measurements were 0.11 and 0.08; the interobserver errors for the MLT and ILT measure-

TABLE I. MANUAL AND AUTOMATED IMC, ML, AND IL SEGMENTATION MEASUREMENTS IN MILLIMETERS FOR ALL SUBJECTS AND FOR THE AGE GROUPS BELOW 50, 50 TO 60, AND ABOVE 60 YEARS OLD.

Set of measurements		Thickness [mm]		se	CV [%]	IMT_{ratio}
		Mean ± sd	Median (IQR)			
1st set of manual measurements at time 0 mo	IMT	0.71 ± 0.17	0.66 (0.18)	0.11	17.3	0.583 ± 0.323
	IMT_50	0.59 ± 0.13	0.57 (0.13)	0.09	14.9	0.431 ± 0.242
	IMT_60	0.74 ± 0.18	0.73 (0.23)	0.12	16.8	0.634 ± 0.273
	IMT_g60	0.82 ± 0.15	0.81 (0.2)	0.10	12.6	0.687 ± 0.273
	MLT	0.25 ± 0.12	0.23 (0.17)	0.09	34	
	MLT_50	0.17 ± 0.09	0.13 (0.15)	0.07	38	
	MLT_60	0.26 ± 0.08	0.26 (0.08)	0.06	23.8	
	MLT_g60	0.31 ± 0.12	0.33 (0.15)	0.1	12.6	
	ILT	0.43 ± 0.10	0.43(0.10)	0.07	16.7	
	ILT_50	0.41 ± 0.05	0.39 (0.09)	0.04	10.0	
	ILT_60	0.43 ± 0.12	0.42 (0.10)	0.08	19.2	
	ILT_g60	0.46 ± 0.08	0.44 (0.06)	0.05	11.4	
2nd set of manual measurements at time 6 mo	IMT	0.72 ± 0.17	0.68 (0.19)	0.12	17.5	0.613 ± 0.307
	IMT_50	0.7 ± 0.2	0.67 (0.26)	0.14	20.2	0.551 ± 0.297
	IMT_60	0.66 ± 0.13	0.63 (0.15)	0.09	14.2	0.652 ± 0.312
	IMT_g60	0.78 ± 0.15	0.73 (0.17)	0.11	14.0	0.632 ± 0.225
	MLT	0.27 ± 0.14	0.25 (0.09)	0.07	9.8	
	MLT_50	0.24 ± 0.12	0.26 (0.21)	0.08	33.5	
	MLT_60	0.25 ± 0.08	0.23 (0.11)	0.11	23.2	
	MLT_g60	0.29 ± 0.12	0.26 (0.13)	0.07	22.4	
	ILT	0.44 ± 0.13	0.44 (0.10)	0.10	21.3	
	ILT_50	0.45 ± 0.14	0.44 (0.10)	0.09	21.1	
	ILT_60	0.41 ± 0.11	0.40 (0.11)	0.10	18.4	
	ILT_g60	0.48 ± 0.11	0.46 (0.08)	0.08	16.1	
Automated segmentation measurements	IMT	0.67 ± 0.12	0.66 (0.12)	0.08	12.6	0.597 ± 0.286
	IMT_50	0.61 ± 0.11	0.59 (0.09)	0.08	12.6	0.461 ± 0.261
	IMT_60	0.68 ± 0.10	0.69 (0.12)	0.07	10.3	0.618 ± 0.236
	IMT_g60	0.74 ± 0.13	0.73 (0.11)	0.1	12.9	0.760 ± 0.320
	MLT	0.25 ± 0.11	0.25 (0.10)	0.08	12.3	
	MLT_50	0.19 ± 0.11	0.17 (0.09)	0.08	14.0	
	MLT_60	0.26 ± 0.10	0.26 (0.12)	0.12	27.1	
	MLT_g60	0.32 ± 0.13	0.11 (0.11)	0.10	29.7	
	ILT	0.42 ± 0.10	0.42(0.90)	0.07	11.7	
	ILT_50	0.25 ± 0.12	0.42(0.90)	0.07	11.7	
	ILT_60	0.25 ± 0.12	0.42(0.90)	0.07	11.7	
	ILT_g60	0.25 ± 0.12	0.42(0.90)	0.07	11.7	

IMC: intima-media complex; IMT: intima-media thickness for all 100 measurements; IMT_50, IMT_60, IMT_g60: IMT values for the age groups below 50, between 50 and sixty, and above 60, respectively; MLT: media layer thickness for all 100 measurements, MLT_50, MLT_60, MLT_g60: MLT values for the age groups below 50, between 50 and sixty, and above 60, respectively; ILT: intima layer thickness for all 100 measurements, ILT_50, ILT_60, ILT_g60: ILT values for the age groups below 50, between 50 and sixty, and above 60, respectively; sd: standard deviation; IQR: inter-quartile range; se: inter-observer error; CV%: coefficient of variation; IMT_{ratio} = MLT/ILT.

ments were 0.09 and 0.08 and 0.07 and 0.07, respectively. The coefficient of variation (CV%), for the manual first set and the automated IMT measurements were 17.3% and 12.6%; the coefficients of variation for the manual first set and the automated MLT and ILT segmentation measurements were 34% and 12.3% and 16.7% and 11.7%, respectively. The IMT_{ratio} for the first set of manual measurements for all 100 images and for the 3 different age groups (below 50, between 50 and 60, and above 60 years old) were 0.5834 ± 0.323 mm, 0.4314 ± 0.242 mm, 0.634 ± 0.273 mm, and 0.6867 ± 0.273 mm, respectively. Similar values, but slightly higher, were observed for the second set of manual measurements carried out at month 6 for the IMT, MLT, and ILT (see Table I). For the IMT_{ratio} using the Wilcoxon rank sum test, there was no significance difference between the automated and the second set of manual measurements ($P = 0.698$), however, there was a significance difference between the automated and the first set of manual measurements ($P = 0.031$) and between the first and second set of manual measurements ($P = 0.011$).

Table II presents the results of the Mann Whitney rank sum test performed between the male and the female subjects for all 3 segmentation measurements (IMT, MLT, ILT) and the IMT_{ratio}. There was no significant difference for the MLT between the male and the female subjects for the first set and automated measurements. Significant differences between male and female subjects were only found for the second set of manual measurements for the IMT ($P = 0.01$) and ILT ($P = 0.013$). There was also no significant difference for the IMT_{ratio} between male and female subjects.

TABLE II. COMPARISON BETWEEN SEX GROUPS (MALE = M, FEMALE = F for the IMC, IM, IL, and $\text{IMT}_{\text{RATIO}}$ USING THE MANN WHITNEY RANK SUM TEST.

	First set of manual measurements				Second set of manual measurements				Automated measurements			
	IMT	MLT	ILT	$\text{IMT}_{\text{ratio}}$	IMT	MLT	ILT	$\text{IMT}_{\text{ratio}}$	IMT	MLT	ILT	$\text{IMT}_{\text{ratio}}$
Sex (M/F)	NS (0.8)	NS (0.193)	NS (0.971)	NS (0.137)	S (0.01)	NS (0.128)	S (0.013)	NS (0.964)	NS (0.362)	NS (0.332)	NS (0.96)	NS (0.362)

IMT: intima-media thickness; MLT: media layer thickness; ILT: intima layer thickness; $\text{IMT}_{\text{ratio}}$: IMT ratio = MLT/ILT. The p value is also shown in parentheses (S = significant difference at $P < 0.05$, NS = nonsignificant difference at $P > 0.05$).

The Wilcoxon rank sum test between the manual and automated IMT, MLT, ILT, and $\text{IMT}_{\text{ratio}}$ measurements was also performed between the 3 different age groups, and it is shown in Table III. The Wilcoxon rank sum test and the correlation coefficient, (with 95% confidence) results performed between the manual and the automated measurements for the IMT, MLT, ILT, and $\text{IMT}_{\text{ratio}}$ showed that there were no significant differences between these sets of measurements.

The automated MLT values (MLT_A) versus age using regression analysis gave an equation of MLT_A = 0.029 + 0.0041*AGE, where the standard error for intercept and slope were 0.0661 and 0.001, respectively. The mean square error due to regression was 0.1509, the residual mean square was 0.013 resulting in an F-ratio of 11.6 with a corresponding significance level of $P = 0.001$. This supports the assumption of a linear relationship between age and MLT. The correlation coefficient was $\rho = 0.33$. It was shown that the MLT at the age of 55 is 0.25 mm and that the 95% confidence interval limits for the MLT are both ± 0.24 mm.

The Bland-Altman plot between the first set of manual measurements and the snakes segmentation MLT measurements showed that the difference between the manual and the snakes segmentation measurements was -0.01 mm with limits of agreement lying between 0.16 mm and -0.18 mm (note that the pixel resolution was 0.08 mm). The Bland-Altman plot between the second set of manual measurements and the snakes segmentation MLT measurements showed that the difference between the manual and the snakes segmentation measurements was 0.01 mm with limits of agreement lying between 0.24 mm and -0.23 mm. The Bland-Altman plot between the first and second set of manual measurements showed that the difference between the first and second set of the manual measurements was -0.02 mm with limits of agreement lying between 0.16 mm and -0.19 mm. There was also a negative bias, as estimated by the mean difference, which showed that on average the snakes segmentation algorithm under estimates the area relative to normal delineation.

Fig. 2 presents box plots of the IMT, MLT, and ILT for the 3 different age groups, extracted from the manual IMC, ML, and IL segmentations for all 100 images of the CCA for the 3 different age groups (below 50, between 50 and 60, and above 60).

IV. DISCUSSION

In this study, both manual and automated IMT, MLT, and ILT measurements are reported for 100 longitudinal ultrasound images of the CCA and their variation with age and sex. The importance of the CCA ML for the evaluation of the risk of CVD was outlined in [2] and shown in [13] that the MLT was thinner for this group of subjects. Also it was shown in [14] that the MLT was strongly related with age for the radial and anterior tibial arteries.

Table I showed that the manual IMT measurements are larger and have a larger range of values, whereas the first set of manual and the automated MLT measurements are almost the same, while the second set of manual measurements were higher. Similar IMT findings were also reported in [9], [10], and [12]. The manual IMT_{mean} plus/minus standard deviation measurements reported in this study (0.71 ± 0.17 mm, 0.72 ± 0.17 mm for manual first and second sets) were larger than the snakes segmented measurements (0.67 ± 0.12 mm), and this finding was also reported in other studies. More specifically, the manual versus the snakes segmented IMT measurements reported in other studies were (0.93 mm vs. 0.88 mm) [9], (0.72 mm vs. 0.63 mm) [11], (0.8 mm vs. 0.7 mm) [12], and (0.92 mm vs. 0.88 mm) [22]. There is a large variation in the IMT measurements between the different studies because different material and different measuring methodologies were used.

The manual first set MLT, ILT measurements, and $\text{IMT}_{\text{ratio}}$ in our study were 0.25 ± 0.12 mm, 0.43 ± 0.10 mm, and 0.5834 ± 0.323 mm, respectively (similar values were obtained for the second set of manual measurements and the automated measurements). In [13], the manual IMT, MLT, and ILT measurements carried out for the CCA by an expert using high-resolution ultrasound with a broadband probe and a 25 MHz center frequency between subjects with and without CVD were 0.75 ± 0.17 mm vs. 0.72 ± 0.20 mm ($P = 0.4$), 0.45 ± 0.14 mm vs. 0.38 ± 0.16 mm ($P < 0.05$), and 0.17 ± 0.006 mm vs. 0.22 ± 0.06 mm ($P < 0.0001$), respectively. It was shown in [13] that subjects with CVD (coronary heart disease, myocardial infarction, or stroke) had a significantly thicker IL and a thinner ML than healthy subjects. The $\text{IMT}_{\text{ratio}}$ also differed significantly between subjects with and without a diagnosis of CVD (0.43 ± 0.20 vs. 0.75 ± 0.48, $P = 0.0002$). The

TABLE III. COMPARISON BETWEEN THE IMC, ML, IL, AND IMT$_{ratio}$ FOR THE MANUAL AND THE AUTOMATED SEGMENTATION MEASUREMENTS BASED ON THE WILCOXON RANK TEST FOR THE THREE DIFFERENT AGE GROUPS, BELOW 50 (< 50), BETWEEN 50 AND 60 (50–60), AND ABOVE 60 (> 60) YEARS OLD.

		Second set of manual measurements												Automated measurements											
		IMT			**MLT**			**ILT**			**IMT$_{ratio}$**			**IMT**			**MLT**			**ILT**			**IMT$_{ratio}$**		
		<50	50–60	>60	<50	50–60	>60	<50	50–60	>60	<50	50–60	>60	<50	50–60	>60	<50	50–60	>60	<50	50–60	>60	<50	50–60	>60
First set of manual measurements																										
IMT	<50	S	NS	S										S	S	S									
	50–60	NS	S	S										S	S	S									
	>60	S	S	NS										S	S	S									
MLT	<50				S	S	S										NS	NS	S						
	50–60				NS	NS	NS										S	S	S						
	>60				NS	S	NS										S	NS	NS						
ILT	<50							S	NS	S										NS	NS	NS			
	50–60							NS	NS	S										NS	NS	NS			
	>60							NS	S	NS										S	S	S			
IMT$_{ratio}$	<50										S	S	S										NS	S	S
	50–60										NS	NS	NS										S	NS	S
	>60										S	NS	NS										S	NS	NS
Second set of manual measurements																										
IMT	<50													S	NS	NS									
	50–60													NS	NS	S									
	>60													S	S	NS									
MLT	<50																S	NS	NS						
	50–60																NS	NS	S						
	>60																S	NS	NS						
ILT	<50																			NS	NS	NS			
	50–60																			NS	NS	NS			
	>60																			S	S	S			
IMT$_{ratio}$	<50																						NS	NS	S
	50–60																						NS	NS	S
	>60																						S	NS	NS

IMT: intima-media thickness; MLT: media layer thickness; ILT: intima layer thickness; IMT ratio = MLT/ILT; S = significant difference at $P < 0.05$; NS = nonsignificant difference at $P > 0.05$.
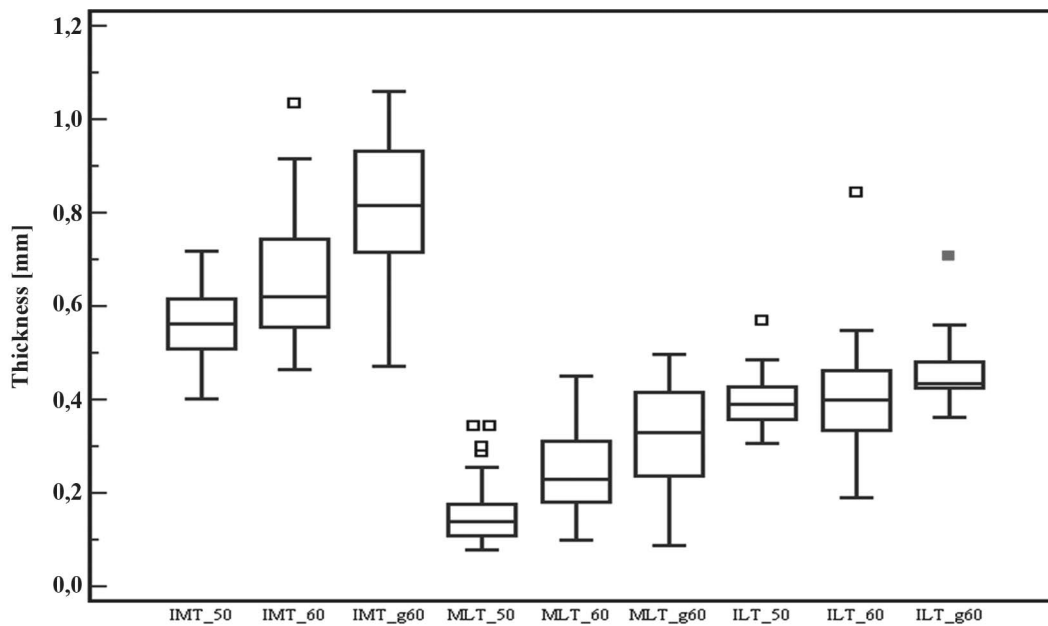
IQR: 0.1257, 0.254, 0.218/0.1577, 0.872, 0.1792/0.0949, 0.1013, 0.0573

Fig. 2. Box plots for the manual measurements of the intima-media thickness (IMT), media layer thickness (MLT), and intima layer thickness (ILT) for the age groups below 50 (50), 50 to 60 (60), and above 60 years (g60) old (i.e., IMT_50, ILT_60, and MLT_g60 represent the values below the age of 50 for IMT, between the ages of 50 and 60 for ILT, and greater than 60 for MLT, respectively).

MLT and ILT were manually measured from the radial and tibial arteries in 90 subjects (10 to 90 years old), using a 55 MHz 2-D ultrasound transducer [14]. The values reported for the MLT ranged from 0.159 ± 0.039 mm to 0.227 ± 0.038 mm, whereas for the ILT values ranged from 0.49 ± 0.08 mm to 0.81 ± 0.019 mm, respectively. Finally, in [8], it was found that the median MLT of muscular arteries was 0.6 mm in the absence of a lesion, decreasing to 0.1 mm in the area of maximal atherosclerosis. The in vivo study was performed in 29 patients undergoing coronary or peripheral vascular procedures using intravascular ultrasound with a 30 MHz frequency ultrasound probe.

It is shown from Table I that, for the MLT measurements, the standard deviation, sd, for the manual (0.12, 0.14 for the first and second set of manual measurements), the automated (0.11), and the coefficient of variation, CV% (34%, 9.8% for the first and second set of manual measurements, and 12.3% for the automated measurements), is large. This is due to the fact that the ML is very small with a complex texture, and therefore, it is very difficult to be estimated correctly either manually or automatically.

Table I also shows that the interobserver errors, se, for the IMT and the MLT, are larger for the manual segmentation measurements (for both the first set and the second set of manual measurements). Also, the results from Table I showed that high intraobserver variabilities occur when manual measurements are made. Smaller values for se were obtained for the automated segmentation measurements, indicating a better performance of the automated versus the manual measurements as documented in [10], [20].

Table II showed that no significant differences were found between men and women for the IMT, MLT, ILT, and the IMT_{ratio}, as also shown in [13], and that the IMT_{ratio} did not differ significantly between male and female groups.

The NS differences between the manual and the automated segmentation method, estimated by the Wilcoxon rank sum test, show that the manual measurements may be replaced by the snakes segmentation measurements with confidence. It was also shown that the manual measurements of the expert at time 0 versus time 6 mo were NS. The correlation coefficient, ρ, showed that the strongest relationship existed between the MLT manual first set and automated segmentation measurements (with $\rho = 0.72$), where higher values were reported. The Wilcoxon rank sum test performed in Table III showed that the first set of manual and automated IMT measurements between all the age groups are mostly significantly different (S), whereas the manual and automated measurements of the MLT and ILT are mostly nonsignificantly different (NS). Furthermore, the Wilcoxon rank sum test for the IMT_{ratio} showed no clear statistical significance between the different age groups; therefore, this measure may not be used as an indicative value for atherosclerotic disease with increasing age.

Based on the Bland Altman test, a small discrepancy of around 0.01 mm was found between the manual and the automated MLT measurements. On this basis, the 2 methods (manual and snakes segmentation) can be considered interchangeable. There are no other studies reported in the literature where Bland-Altman plots were used for

comparing the manual and automated MLT measurements. The Bland-Altman plot was used in [22], where 24 carotid ultrasound images were analyzed by 2 experts for validating the results of IMT measurements using a newly developed system by comparing them with those obtained using previous methods and showed no evidence of bias between the 2 methods.

This study shows that there might be a linear relationship between MLT-automated measurements and age, where all measurements showed an increase with age. Similar findings were also reported for the IMT in [10]. It was also shown that in this study the values of the mean IMT in a carotid artery vary between 0.54 mm and 0.88 mm, depending on age, and this is also consistent with other studies [2], [6], [12], [23], whereas the values of the MLT vary between 0.13 mm to 0.37 mm. Furthermore, in [14], the IMT, MLT, and ILT of 90 healthy subjects (aged between 10 and 90 years) were manually measured at their radial and anterior tibial artery. It was shown that age was strongly related with IMT, MLT, and ILT of both peripheral arteries.

The normalization method used in this study was documented to be helpful in the manual contour extraction [24] as well as the snakes segmentation of the IMC [10] and the atherosclerotic carotid plaque segmentation [25]. In addition, this method increased the classification accuracy of different plaque types as assessed by the experts [26]. Ultrasound image normalization was carried out before segmentation of the IMT in [27] where histogram equalization was performed on carotid artery ultrasound images for increasing the image contrast.

It has been demonstrated in [2] and [28] that the blood/endothelium (intima) interface and the media-adventitia interface correspond to their anatomical/histological counterparts. This is not the case with the intima-media interface because the width of the white band closer to the lumen is gain dependent and therefore variable. Thus, the measurement of the MLT represents only an ultrasonic measurement (as also discussed above). It should be noted, however, that part of the ML, shown in ultrasound image as an echolucent band, shown in Fig. 1(a), band Z6, contains the hypoechoic muscular arterial tunica media and perhaps the hypoechoic part of the arterial tunica intima. It is well known that atherosclerosis causes an increase of the arterial tunica intima thickness. As has been also reported earlier in the literature [11], the histological boundaries between the arterial tunica intima and media (internal elastic lamina) in ultrasound images cannot be accurately delineated. Therefore, we hypothesize that the increase of the MLT with age as reported in our study (see also [10]) may be a misleading finding, because part of the ML as shown in ultrasound images may belong to the arterial tunica intima. We recommend that the above hypothesis should be taken into account in future work studying the ML texture and morphology. It should be furthermore noted that there are no other studies reported in the literature where ML

segmentation and measurements were performed on longitudinal ultrasound images of the CCA.

A limitation of the proposed method is that the manual and automated ML and IL segmentation measurements were performed in linear segments of the CCA because in the clinical praxis, the experts are delineating the IMC and the ML only in those parts of the vessel where there are no significant artifacts, signal drop outs, and structure irregularities [2], [9], [10], [18], [26], [29].

Another limitation of the proposed method is the presence of acoustic shadowing together with strong speckle noise, which hinders the visual and automatic analysis in ultrasound images [9], [10]. Such images, as well as images with extensive echolucency and calcification where the ML was not well visually recognized, were excluded from the study. Backscattered ultrasound is also angle dependent. During the recording of the images, a standard recording technique was used to adjust the position of the probe so that the ultrasound beam was at right angles to the arterial wall. This improved the IMC visualization. In addition, the new spatial compound imaging technique might optimize further carotid ultrasound imaging [24], [26]. The small size of the ML and the estimation and positioning of the initial snake contour may sometimes result in segmentation errors. This should be placed as close as possible to the area of interest, otherwise it may be trapped into local minima or false edges and converge to a wrong location.

As it has already been mentioned in Section II-A, the axial resolution of the system used, was 0.11 mm, which indicates that structures greater than 0.11 mm can be correctly visualized and measured (see also [30]). In addition, it is noted that the pixel resolution was 0.06 mm. For structures thinner than 0.11 mm, the 2 echo interfaces (i.e., of ML) cannot be separated, and measurements of these structures are not possible. For the data set investigated in this study, 6% of the measurements were below 0.11 mm, therefore, these measurements may be considered as unreliable. It should be noted, however, that with new ultrasound equipment and new probes that are available having a recording frequency in the range of 15 MHz, this problem would be highly limited. In another study where the variability of the IMT between experts and between manual and automated IMT measurements was investigated [30], it was shown that the reproducibility of the IMT measurements may be further improved if the IMT mean value is computed from multiple ultrasound images (frames) of the carotid, instead of the mean value obtained from only one frame [30]. These can be also investigated in a future study for the case of the MLT and ILT measurements.

In the present study, in less than 8% of the cases, the positioning of the initial snake contour was not calculated correctly. Furthermore, there were also another 6% of the cases where the ML structure was very small and the 2 snake contours were trapped together. For these cases, the user of the proposed system may run the snake's initialization procedure again to estimate the correct initial

snake contour, and during the snake's deformation, the user may interact and manually correct the contour.

V. Conclusion and Future Work

It was clearly illustrated in this study that both manual and automated IMT, MLT, and ILT measurements could be carried out successfully. Also, it was shown that there was overall no significant difference between the manual and the automated measurements and between the male and female subjects. It was also shown that these values (manual and automated measurements) increase with age.

The segmented IMC, ML, and IL bands may be used for extracting texture features [31], which might be able to differentiate between subjects with high and low risk of stroke. Furthermore, the change of these textural characteristics with age may give additional information for characterizing subjects in different risk groups. In a recent study [29], it was shown that the gray scale median of the IMC of the CCA is closely related to the echogenecity in overt carotid plaques. This finding suggests that the gray scale median and other texture features extracted from the IMC or the ML bands could have prognostic impact for the assessment of cardiovascular risk. However, the IMT_{ratio} was not found to be statistically significant different with increasing age.

Risk factors like smoking, blood pressure, inflammation markers, and cholesterol correlate to the traditional carotid IMT [1], [3], [4], [14]. It would have been valuable to relate these risk factors to IMT, MLT, and ILT measurements. Ongoing studies from our group will provide more data on this topic.

The methodology presented in this study will be further evaluated on ultrasound images of the CCA collected on a large-scale epidemiological study by our group as well as for the segmentation and measurement of curved segments of the bifurcation bulb of the CCA.

References

[1] American Heart Association, Heart disease and stroke statistics—2008, update, Dallas, Texas, 2007. [Online]. Available: http://www.americanheart.org/presenter.jhtml.

[2] P. Pignoli, E. Tremoli, A. Poli, P. Oreste, and R. Paoleti, "Intima plus media thickness of the arterial wall: A direct measurement with ultrasound imaging," *Atheroscl.*, vol. 74, no. 6, pp. 1399–1406, 1986.

[3] P.-J. Touboul, J. Labreuche, E. Vicaut, and P. Amarenco, "Carotid intima-media thickness, plaques, and Framingham risk score as independent determinants of stroke risk," *Stroke*, vol. 36, no. 8, pp. 1741–1745, 2005.

[4] T. Watanabe, S. Koba, M. Kawamura, M. Itokawa, T. Idei, Y. Nakagawa, T. Iguchi, and T. Katagiri, "Small dense low-density lipoprotein and carotid atherosclerosis in relation to vascular dementia," *Metabolism*, vol. 53, no. 4, pp. 476–482, 2004.

[5] C. D. Mario, G. Gorge, R. Peters, F. Pinto, D. Hausmann, C. von Birgelen, A. Colombo, H. Murda, J. Roelandt, and R. Erbel, "Clinical application and image interpretation in coronary ultrasound.

Study group of intra-coronary imaging of the working group of coronary circulation and of the subgroup of intravascular ultrasound of the working group of echocardiography of the European Society of Cardiology," *Eur. Heart J.*, vol. 19, no. 2, pp. 201–229, 1998.

[6] M. L. Grønholdt, B. G. Nordestgaard, T. V. Schroeder, S. Vorstrup, and H. Sillensen, "Ultrasonic echolucent carotid plaques predict future strokes," *Circulation*, vol. 104, no. 1, pp. 68–73, Jul. 2001.

[7] J. E. Wilhjelm, M. L. M. Grønholdt, B. Wiebe, S. K. Jespersen, L. K. Hansen, and H. Sillensen, "Quantitative analysis of ultrasound B-mode images of carotid atherosclerotic plaque: Correlation with visual classification and histological examination," *IEEE Trans. Med. Imaging*, vol. 17, no. 6, pp. 910–922, Dec. 1998.

[8] E. J. Gussenhoven, P. A. Frietman, S. H. The, R. J. van Suylen, F. C. van Egmond, C. T. Lancée, H. van Urk, J. R. Roelandt, T. Stijnen, and N. Bom, "Assessment of medial thinning in atherosclerosis by intravascular ultrasound," *Am. J. Cardiol.*, vol. 68, pp. 1625–1632, Dec. 1991.

[9] I. Wendelhag, Q. Liang, T. Gustavsson, and J. Wikstrand, "A new automated computerized analysing system simplifies reading and reduces the variability in ultrasound measurement of intima media thickness," *Stroke*, vol. 28, pp. 2195–2200, Nov. 1997.

[10] C. P. Loizou, C. S. Pattichis, M. S. Pantziaris, T. Tyllis, and A. N. Nicolaides, "Snakes based segmentation of the common carotid artery intima media," *Med. Biol. Eng. Comput.*, vol. 45, pp. 35–49, Jan. 2007.

[11] M. Gutierrez, P. Pilon, S. Lage, L. Kopel, R. Carvalho, and S. Furuie, "Automatic measurement of carotid diameter and wall thickness in ultrasound images," *Comput. Cardiol.*, vol. 29, pp. 359–362, Sep. 2002.

[12] S. Delsanto, F. Molinari, P. Giustetto, W. Liboni, S. Badalamenti, and J. S. Suri, "Characterization of a completely user independent algorithm for carotid artery segmentation in 2-D ultrasound images," *IEEE Trans. Instrum. Meas.*, vol. 56, no. 4, pp. 1265–1274, 2007.

[13] K. A. Rodriguez-Maciasa, L. Lindbc, and T. Naessena, "Thicker carotid intima layer and thinner media layer in subjects with cardiovascular diseases: An investigation using noninvasive high-frequency ultrasound," *Atheroscl.*, vol. 189, no. 2, pp. 393–400, 2006.

[14] W. Osika, F. Dangardt, J. Grönros, U. Lundstam, A. Myredal, M. Johansson, R. Volkmann, T. Gustavsson, L. M. Gan, and P. Friberg, "Increasing peripheral artery intima thickness from childhood to seniority," *Arterioscler. Thromb. Vasc. Biol.*, vol. 27, pp. 671–676, Dec. 2007.

[15] G. S. Mintz, S. E. Nissen, W. Anderson, S. R. Bailey, R. Erbel, P. J. Fitzgerald, F. J. Pinto, K. Rosenfield, R. J. Siegel, and E. M. Tuzcu, and P. G. Yock, "American college of cardiology clinical expert consensus document on standards for acquisition, measurements and reporting intravascular ultrasound studies (IVUS)," *J. Am. Coll. Cardiol.*, vol. 37, pp. 1478–1492, Apr. 2001.

[16] C. P. Loizou, C. S. Pattichis, M. Pantziaris, A. Nicolaides, N. Georgiou, and E. Kyriakou, "Media thickness measurement of the common carotid artery," in *Proc. IEEE EMBS 2007, 29th Ann. Int. Conf. IEEE Engineering in Medicine and Biology*, Lyon, France, Aug. 23–26, 2007, FrP1B6.5, pp. 2171–2174.

[17] E. Kyriakou, M. S. Pattichis, C. H. Christodoulou, C. S. Pattichis, S. Kakkos, M. Griffin, and A. N. Nicolaides, "Ultrasound imaging in the analysis of carotid plaque morphology for the assessment of stroke," in *Plaque Imaging: Pixel to Molecular Level*, J. S. Suri, C. Yuan, D. L. Wilson, S. Laxminarayan, Eds. Amsterdam, The Netherlands: IOS Press, 2005, pp. 241–275.

[18] T. J. Tegos, M. M. Sabetai, A. N. Nicolaides, T. S. Elatrozy, S. Dhanjil, and J. M. Stevens, "Patterns of brain computed tomography infraction and carotid plaque echogenicity," *J. Vasc. Surg.*, vol. 33, pp. 334–339, Feb. 2001.

[19] D. J. Williams and M. Shah, "A fast algorithm for active contour and curvature estimation," *Comput. Vis. Image Underst.*, vol. 55, no. 1, pp. 4–26, 1992.

[20] V. Chalana and Y. Kim, "A methodology for evaluation of boundary detection algorithms on medical images," *IEEE Trans. Med. Imaging*, vol. 16, no. 5, pp. 642–652, Oct. 1997.

[21] J. M. Bland and D. G. Altman, "Statistical methods for assessing agreement between two methods of clinical measurement," *Lancet*, vol. 1, no. 8476, pp. 307–310, Feb. 1986.

[22] G. B. J. Mancini, D. Abbott, C. Kamimura, and E. Yeoh, "Validation of a new ultrasound method for the measurement of carotid

artery intima medial thickness and plaque dimensions," *Can. J. Cardiol.*, vol. 20, no. 13, pp. 1355–1359, Nov. 2004.

[23] S. Graf, J. Gariery, M. Massonneau, R. Armentano, S. Mansour, J. Barra, A. Simon, and J. Levenson, "Experimental and clinical validation of arterial diameter waveform and intimal media thickness obtained from B-mode ultrasound image processing," *Ultrasound Med. Biol.*, vol. 25, no. 9, pp. 1353–1363, Nov. 1999.

[24] C. P. Loizou, C. S. Pattichis, M. S. Pantziaris, T. Tyllis, and A. N. Nicolaides, "Quantitative quality evaluation of ultrasound imaging in the carotid artery," *Med. Biol. Eng. Comput.*, vol. 44, no. 5, pp. 414–426, May 2006.

[25] C. P. Loizou, C. S. Pattichis, M. S. Pantziaris, and A. N. Nicolaides, "An integrated system for the segmentation of atherosclerotic carotid plaque," *IEEE Trans. Inf. Technol. Biomed.*, vol. 11, no. 5, pp. 661–667, Nov. 2007.

[26] A. N. Nicolaides, S. K. Kakkos, M. Griffin, M. Sabetai, S. Dhanjil, D. Thomas, G. Geroulakos, N. Georghiou, S. Francis, E. Ioannidou, and C. Dorě, "Effect of image normalization on carotid plaque classification and the risk of ipsilateral hemispheric events: Results from the asymptomatic carotid stenosis and risk of stroke study," *Vascular*, vol. 1, no. 4, pp. 211–221, 2005.

[27] A. Mojsilovic, M. Popovic, N. Amodaj, R. Babic, and M. Ostojic, "Automatic segmentation of intravascular ultrasound images: A texture based approach," *Ann. Biomed. Eng.*, vol. 25, pp. 1059–1071, Nov.–Dec. 1997.

[28] G. Belcaro, A. N. Nicolaides, G. Laurora, M. R. Cesarone, M. De Sanctis, L. Incandela, and A. Barsotti, "Ultrasound morphology classification of the arterial wall and cardiovascular events in a 6-year follow-up study," *Arterioscler. Thromb. Vasc. Biol.*, vol. 16, pp. 851–856, Jul. 1996.

[29] L. Lind, J. Andersson, M. Roenn, and T. Gustavsson, "The echogenecity of the intima-media complex in the common carotid artery is closely related to the echogenecity in plaques," *Atheroscl.*, vol. 195, pp. 411–414, 2007.

[30] C. Schmidt and I. Wendelhag, "How can the variability in ultrasound measurements of intima-media thickness be reduced? Studies of interobserver variability in carotid and femoral arteries," *Clin. Physiol.*, vol. 19, no. 1, pp. 45–55, Jan. 1999.

[31] C. I. Christodoulou, C. S. Pattichis, M. S. Pantziaris, and A. N. Nicolaides, "Texture-based classification of atherosclerotic carotid plaques," *IEEE Trans. Med. Imaging*, vol. 22, no. 7, pp. 902–912, Jul. 2003.

Constantinos S. Pattichis (S'88–M'88–SM'99) was born in Cyprus on January 30, 1959, and received his diploma as technician engineer from the Higher Technical Institute in Cyprus in 1979, the B.Sc. in Electrical Engineering from the University of New Brunswick, Canada, in 1983, the M.Sc. in Biomedical Engineering from the University of Texas at Austin in 1984, the M.Sc. in Neurology from the University of Newcastle Upon Tyne, UK, in 1991, and the Ph.D. in Electronic Engineering from the University of London, UK, in 1992. He is currently Professor with the Department of Computer Science of the University of Cyprus. His research interests include e-health, medical imaging, biosignal analysis, and intelligent systems.

He has been involved in numerous projects in these areas funded by EU, the National Research Foundation of Cyprus, the INTERREG and other bodies, such as the INTRAMEDNET, INTERMED, FUTURE HEALTH, AMBULANCE, EMERGENCY, ACSRS, TELEGYN, HEALTHNET, IASIS, IPPOKRATIS, and others with a total funding managed close to 5 million Euros. He has published 50 refereed journal and 130 conference papers, and 19 chapters in books in these areas. He is Co-Editor of the books *M-Health: Emerging Mobile Health Systems*, published in 2006 by Springer and of *Information Technology in Biomedicine*, to be published in 2009 by IEEE. He is co-author of the monograph *Despeckle Filtering Algorithms and Software for Ultrasound Imaging*, published by Morgan & Claypool Publishers in 2008. He was Guest Co-Editor of the Special Issues on Emerging Health Telematics Applications in Europe, and of the forthcoming Emerging Technologies in Biomedicine, and Computational Intelligence in Medical Systems of the *IEEE Transactions on Information Technology in Biomedicine*. He was General Co-Chairman of the Medical and Biological Engineering and Computing Conference (MEDICON'98), and the IEEE Region 8 Mediterranean Conference on Information Technology and Electrotechnology (MELECON'2000); Program Co-Chair of the IEEE Information Technology in Biomedicine, ITAB06; and General Co-Chair of ITAB09 to be organised in Cyprus. Moreover, he served as an Associate Editor of the *IEEE Transactions on Information Technology* in Biomedicine and the *IEEE Transactions on Neural Networks*. He served as Chairperson of the Cyprus Association of Medical Physics and Biomedical Engineering (1996–1998), and the IEEE Cyprus Section (1998–2000). He is a Senior Member of IEEE.

Christos P. Loizou is an assistant professor in computer science. He received his B.Sc. degree in electrical engineering and the Dipl.-Ing. (M.Sc.) degree in computer science and telecommunications from the University of Kaisserslautern, Kaisserslautern, Germany, and the Ph.D. degree from the Department of Computer Science, Kingston University, London, UK, on ultrasound image analysis of the carotid artery in 1986, 1990, and 2005, respectively. From 1996 to 2000, he was a lecturer in the Department of Computer Science, Higher Technical Institute, Nicosia, Cyprus. Since 2000, he has been an assistant professor in the Department of Computer Science of the School of Sciences and Engineering, Intercollege, Cyprus. He also served as a manager of a telecommunications company from 1990 to 1996. He has served as a supervisor of a number of Ph.D. and B.Sc. students in the area of computer image analysis and telemedicine. He has published 1 book, 5 chapters in books, 7 refereed journal articles, and 25 conference proceeding papers. His current research interests include medical imaging and processing, motion and video analysis, signal and image processing, pattern recognition, biosignal analysis, in ultrasound, magnetic resonance, and optical coherence tomography imaging and computer applications in medicine. Dr. Loizou is a member of the IEEE and a Senior Member of the IEE. He is also an associated researcher at the Institute of Neurology and Genetics in Nicosia, Cyprus. He serves as a reviewer for many IEEE Transaction journals and served as a chair and co-chair at many IEEE conferences. He received funding for different research projects supported by the Institute of Promotion and Foundation in Cyprus, which exceeds 1,500,000 Euros. His research work has been supported by various research grants and has been published in international conference proceedings and journals.

Andrew N. Nicolaides (MS, FRCS, FRCSE) is a graduate of Guy's Hospital Medical School (London University, 1962), and a fellow of the Royal College of Surgeons, England, and the Royal College of Surgeons, Edinburgh (1967).

His higher surgical training was in Oxford University, Kings College Hospital Medical School and St. Mary's Hospital Medical School, London. He was awarded the Jacksonian prize by the Royal College of Surgeons, England, in 1972 for his work on the prevention of venous thromboembolism and obtained the degree of M.S. (Master of Surgery) in 1976.

He was professor of vascular surgery at the Imperial College School of Medicine (St. Mary's Hospital) and consultant vascular surgeon at St. Mary's Hospital from 1983 to 2000 and medical director of the Cyprus Institute of Neurology and Genetics from 2001 to 2004. His research group is known internationally in several areas, which include noninvasive vascular screening and diagnostic investigation and early detection and prevention of cardiovascular and venous disease. His research is now directed toward the genetic risk factors for cardiovascular disease, identification of individuals at risk, and the development of effective methods of prevention, especially stroke.

He is past president of the International Union of Angiology and past president of the Section of Measurement in Medicine of the Royal Society of Medicine.

He has received many awards and honorary memberships from many scientific societies. He is editor-in-chief of *International Angiology* and is on the Editorial Board of many vascular journals. He is Professor Emeritus at Imperial College and an examiner for M.S. and Ph.D. degrees for London University. He is a "Special Scientist" at the University of Cyprus and medical director of the Vascular Screening and Diagnostic Centre in London. He is chairman of the board of European Venous Forum and member of the Angiology Forum of the RSM. He has trained more

than 200 vascular surgeons who are practicing all over the world; twelve of them are holding prestigious chairs as professors in vascular surgery.

He was made Archon Megas Referendarios, an honor bestowed by the Patriarch of Constantinople in 1994. He is co-author of more than 500 original papers and editor of 14 books.

Marios Pantziaris received the M.D. degree in neurology from the Aristotelion University, Thessaloniki, Greece, in 1995. Currently, he is working with Cyprus Institute of Neurology and Genetics, Nicosia, Cyprus, as a senior neurologist in the Neurological Department and is the head of the Neurovascular Department. He was trained in Carotid Duplex–Doppler ultrasonography at St. Mary's Hospital, London, in 1995. In 1999, he was a visiting doctor in acute stroke treatment at Massachusetts General Hospital, Harvard University, Boston, MA. He has considerable experience in carotid–transcranial ultrasound, has participated in many research projects, and has several publications to his name. He is also the head of the Multiple Sclerosis (MS) Clinic where he is running research projects studying the etiology and therapy of MS.